

Carbon Pool Detection Through GIS Techniques and Satellite Data in a Semi Urban Region



Thiyam Tamphasana Devi and A. Abdulla Azaruden

1 Introduction

Carbon which is an important element required by all the living things on earth is stored in different places and in different forms. Thus, the amount of carbon stored in a system is known as “Carbon Stock” of Carbon Pool”. Carbon sequestration is a phenomenon for the storage of CO₂ or other forms of carbon to mitigate global warming. There are major carbon pools i.e., ocean, soil, atmosphere, and forests. In forest ecosystem carbon is stored as aboveground biomass (leaves, trunks, limbs), belowground biomass (roots), deadwood, litter (fallen leaves, stems), and soils. For mitigation of climate change and global warming, sustainable management of carbon pools is important [1–3]. Various human activities like afforestation and soil degradation constantly cause reductions in carbon stock and its sequestration. Thus, several researchers studied carbon stock and its sequestration through forest [4, 5] and soils [6, 7]. Ray et al. [8] did a study on estimation of carbon stock and sequestration at the mangrove forest of Sundarbans in the Bay of Bengal, India. They observed that carbon stock is lower in the tropical mangrove forest than in the terrestrial tropical forest and their annual increase exhibits faster turnover than the tropical forest. Feng et al. [9] studied soil carbon stock and its sequestration in China. They conclude that accumulation of soil carbon stock will not necessarily increase the amount of decomposition in warm climate; however, it will increase the productivity of crop land and its ecosystem functions. The integrated approach of GIS (Geographical Information System) techniques with satellite data is highly potential to generate reliable information on natural ground surface data i.e., land surface temperature, LULC (landcover/landuse), NDVI (normalized difference vegetation index). Using this generated information carbon stock [10] and its sequestration [11] can be calculated and is used for its sustainable management [12–14]. Bordoloi et al. [14] conducted a study to model

T. T. Devi (✉) · A. A. Azaruden
Department of Civil Engineering, National Institute of Technology, Manipur 795004, India
e-mail: thiyam85@gmail.com

the carbon stock and its sequestration using integrated approach of GIS techniques with satellite data in North Eastern part of India. They have shown that the use of different optical satellite derived vegetation index i.e., NDVI, SAVI (soil adjusted vegetation index), ARVI (atmospherically resistant vegetation index), and empirical modeling approach in the study is effective. In this present study, estimation of carbon stock and its sequestration is conducted in Imphal west district of Manipur state using integrated approach of GIS techniques with satellite data and open source tool InVEST model v3.5.0 (Integrated Valuation of Ecosystem Services and Trade-offs) for different types of LULC (landuse/landcover).

2 Study Area

The location of study area (Imphal West district) is provided in Fig. 1. The area of the district measured 558 Km² and it lies at a latitude of 24.30–25.00N and longitude of 93.45–94.15E. Imphal West has the highest population of 2,21,422 among the other district of the state Manipur. And most of the time, it enjoys the comfortable weather.

3 Data and Tools

The data used with its source of collection and extraction is provided in Table 1. Soil map prepared by National Bureau of Soil Survey & Land Use Planning (NBSS & LUP) on 1:500,000 scale was used for extraction of physical and chemical properties of soil viz. soil depth, soil texture, soil drainage, and soil erosion. Default carbon value is prepared by Intergovernmental panel for climate change based upon that holding capacity in different pools like Above ground biomass, Below ground biomass, Soil carbon, Dead wood, and Harvest wood products. LULC is generated from Landsat 5 TM and Landsat 8 OLI for the years 1996 and 2016 respectively by maximum likelihood supervised classification with the help of ArcGIS[®] software.

The elevation, slope and aspect map for the study area were generated from SRTM-DEM (shuttle radar topography mission—digital elevation model) (30 m resolution). Prediction of future LULC for the year 2026 was achieved through GeoSOS-FLUS (geographical simulation and optimization system—future land use simulation) which consists of two main parts as ANN-based (artificial neural networks) probability-of occurrence estimation module; and self-adaptive inertia and competition mechanism CA (cellular automata) module. In this study, ANN-based probability of occurrence estimation module was adopted. The input parameter used is aspect, elevation, slope, euclidian distance to Road, euclidian distance to settlement, and existing LULC (historical) map. Aspect and Slope for the district are obtained from DEM imagery which is taken from SRTM satellite. GeoSOS- FLUS software consists of two main parts. By using LULC and the default carbon value map carbon stock and carbon sequestration map were obtained.

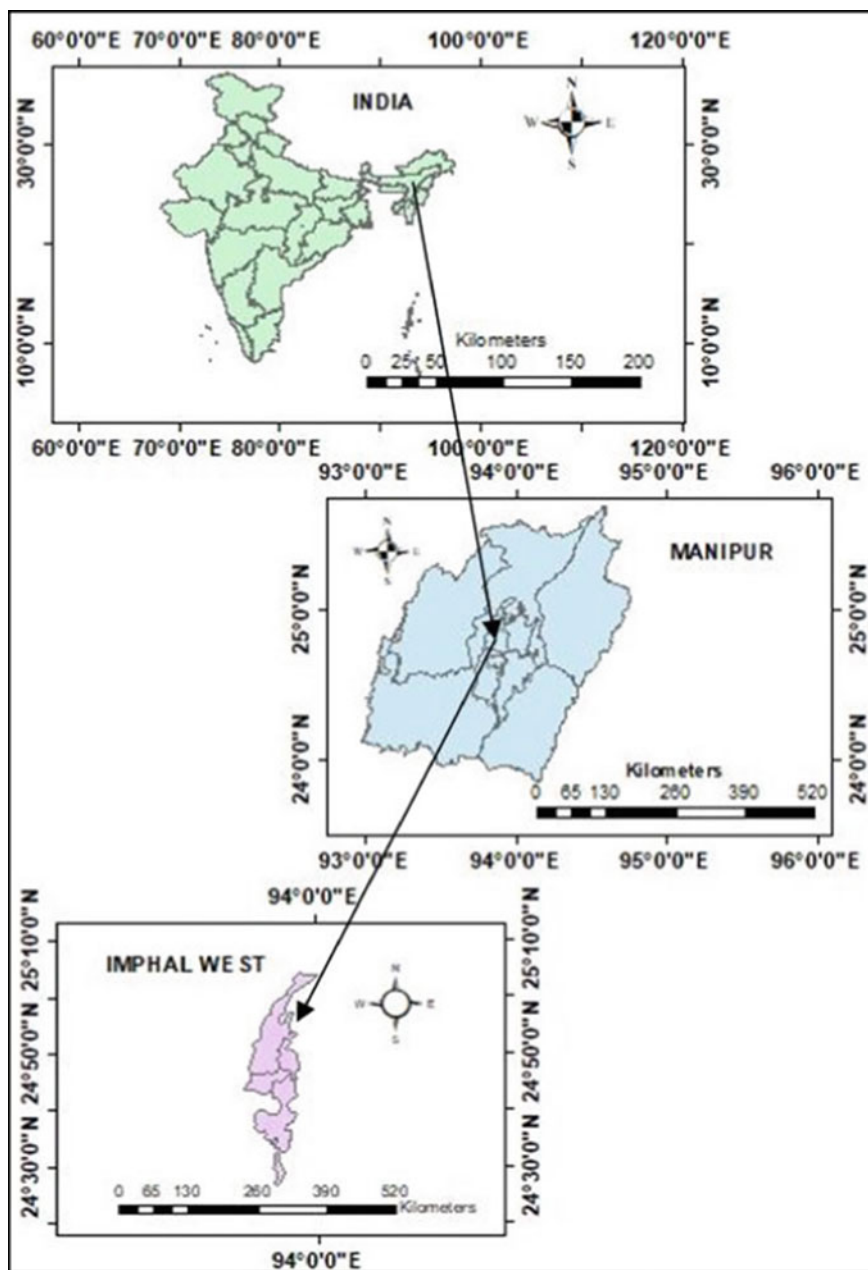


Fig. 1 Study area

Table 1 Data used in the study

Sl. no.	Data	Source	Generated data type
1	Soil map	NBSSLUP, Nagpur	Soil type
2	Landsat 8 OLI (Dated 17/01/2016), Landsat 5 TM (Dated 11/02/1996)	USGS	Land surface temperature and LULC
3	STRM-DEM (30 m resolution)	USGS	Slope and Aspect
4	Geological map	Geological Survey of India (GSI)	
5	Default carbon value	Intergovernmental panel for climate change (IPCC)	Default carbon value for different LULC

4 Equations

4.1 Land Surface Temperature

It is calculated as:

$$\text{Land surface temperature} = \frac{\text{Brightness temperature}}{\left[1 + \left(\frac{0.00115 \times \text{Brightness temperature}}{0.4388} \right) \times \ln(\text{land surface temperature}) \right]} \quad (1)$$

$$\text{Brightness temperature} = \frac{Y_2}{\ln\left[\left(\frac{Y_1}{\text{TOA}}\right) + 1\right]} - 273.15 \quad (2)$$

where, Y_1 & Y_2 are the thermal conversion constant and TOA is the Top of Atmospheric spectral radiance and is calculated as:

$$\text{TOA} = X_L \times P_{\text{cal}} + R_L \quad (3)$$

where, X_L is the band-specific multiplicative rescaling factor, P_{cal} corresponds to band 10, R_L is the band-specific additive rescaling factor.

Then, land surface emissivity is calculated as:

$$\text{Land surface emissivity} = 0.004 \times \text{Proportion to vegetation} + 0.986 \quad (4)$$

Proportion of vegetation is calculated as:

$$\text{Proportion of vegetation} = \left(\frac{\text{NDVI} - \text{NDVIs}}{\text{NDVIv} - \text{NDVIs}} \right)^2 \quad (5)$$

$$\text{NDVI is given as: } \text{NDVI} = \frac{(\text{NIR} - \text{RED})}{(\text{NIR} + \text{RED})}. \quad (6)$$

4.2 Accuracy Assessment for LULC

Accuracy of the classified feature is measured by the overall accuracy (OA) and Kappa coefficient (K) and is calculated as:

$$\text{OA} = \left(\frac{\text{Summation of all Total number Correctly Classified Samples}}{\text{Total Numbers of Samples}} \right) \times 100\% \quad (7)$$

$$\text{K} = \frac{(\text{Observed Accuracy} - \text{Chance Agreement})}{(1 - \text{Chance Agreement})} \quad (8)$$

If $\text{K} < 0.4$ poor, $0.4 < \text{K} < 0.75$ good, $\text{K} > 0.75$ excellent.

4.3 Carbon Stock and Sequestration Model

The default values of carbon values (Intergovernmental panel for climate change, IPPC) for different carbon pools are provided in Table 2 for different LULC types.

The carbon stock $\text{CS}_{x(i,j)}$ in a grid cell (i, j) is estimated as:

$$\text{CS}_{x(i,j)} = A \left[\begin{array}{l} (\text{CS_above})\text{CS}_{x(i,j)} + (\text{CS_below})\text{CS}_{x(i,j)} \\ + (\text{CS_soil})\text{CS}_{x(i,j)} + (\text{CS_dead})\text{CS}_{x(i,j)} \end{array} \right] \quad (9)$$

where, A is the area of the cell; C_above, C_below, C_soil, and C_dead are the above ground carbon, below ground carbon density, soil organic carbon density, and dead organic matter carbon stock. Total carbon stock (CS) and its sequestration (SS) are

Table 2 Default carbon value (IPPC)

Classes	C_above (Mg/ha)	C_below (Mg/ha)	C_soil (Mg/ha)	C_dead (Mg/ha)
Dense forest	140	70	35	12
Sparse forest	65	40	25	6
Crop land	23	35	30	5
Scrub/grass	30	30	30	13
Built-up	4	5	15	1
Water bodies	0	0	0	0

then estimated as:

$$CS = \sum_{x=1}^n CS_{x(i,j)} \tag{10}$$

$$SS = CS^{p_2} - CS^{p_1} \tag{11}$$

where, C^{p_2} and C^{p_1} are the carbon stocks of p_2 and p_1 year respectively.

5 Results and Discussion

5.1 NDVI

It is noted (Fig. 2) that in the year 1996 to year 2016, there is a change in vegetation which shows a decrease in the vegetation cover during the last decade and its responses to climatic parameters. In the year 1996, the vegetation dynamics ranges from -0.1561 to 0.6521 and the density is decreasing in the year 2016 ranging from -0.3636 to 0.6418 . It shows due to climatic parameter change vegetation dynamics also respond.

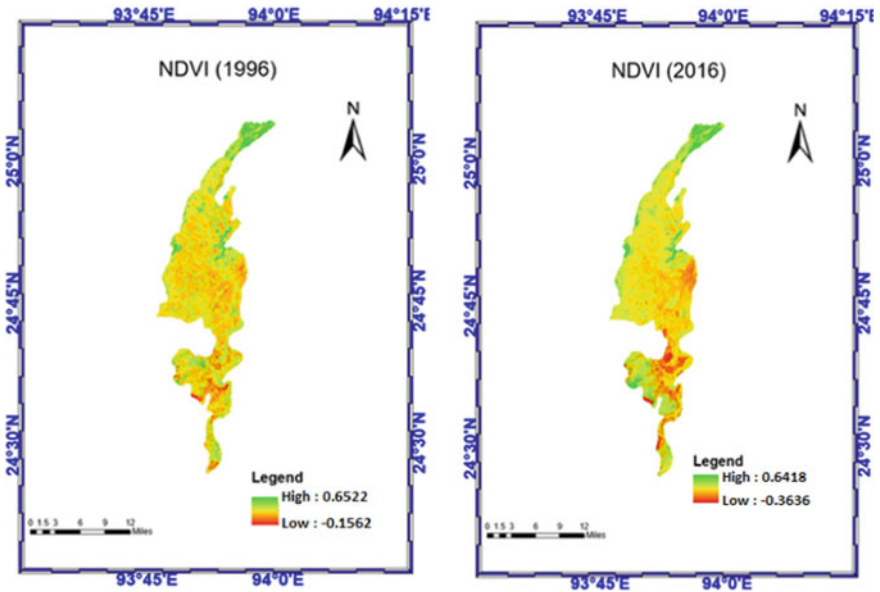


Fig. 2 NDVI of Imphal west district in year 1996 (left) and 2016 (right)

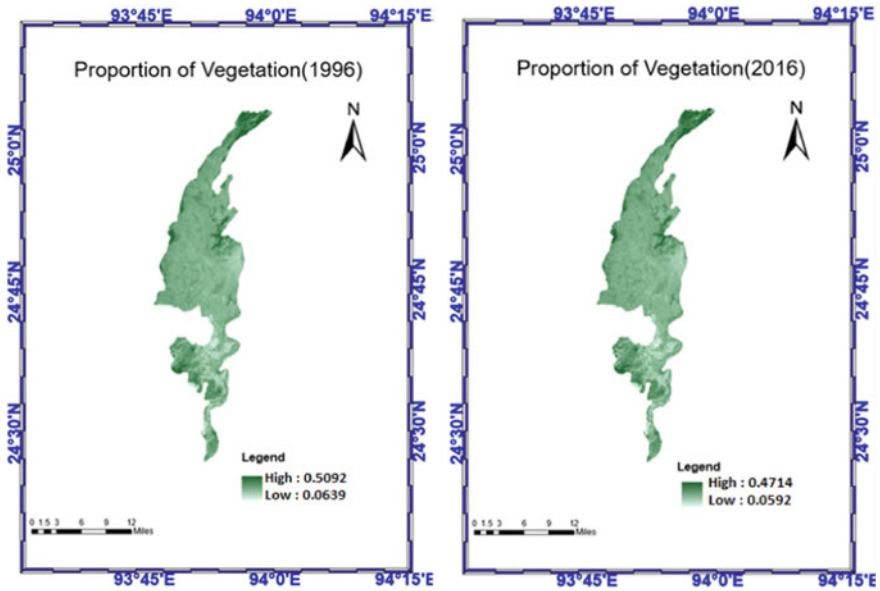


Fig. 3 Proportion of vegetation in the years 1996 (left) and 2016 (right)

5.2 Proportion of Vegetation

In the year 1996 to year 2016 there is a change in vegetation and it decreases in the vegetation cover during the last decade and its responses to climatic parameters (Fig. 3). In the year 1996 the proportion of vegetation ranges from 0.0639 to 0.5091 and the proportion is decreasing in the year 2016 ranging from 0.05919 to 0.4714. This will affect surface emissivity. This enormous variation will affect the carbon holding capacity of the vegetation and it lead the chance to global warming and climate change.

5.3 Land Surface Emissivity

Figure 4 shows the difference in emissivity during the year 1996 (Fig. 4 left) and year 2016 (Fig. 4 right).

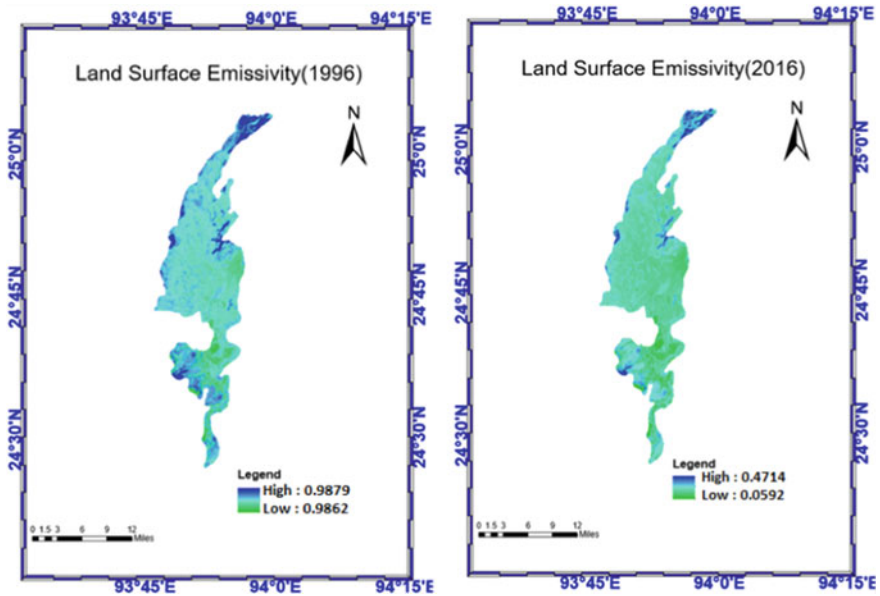


Fig. 4 Land surface emissivity in the years 1996 (left) and 2016 (right)

5.4 Land Surface Temperature

Land surface temperature for the year 1996 and year 2016 is shown in Fig. 5. Here, it shows that the temperature variation depends on the vegetation dynamics. The LST is high in urban places with 20.4 °C and low at forest areas with 9.93 °C in the year 1996 and 22.1 and 10.7 °C in the year 2016 respectively.

5.5 LULC

LULC for the years 1996 and 2016 are shown in Fig. 6 and is classified as dense forest, sparse forest, scrub/grass, crop land, built-up, and water bodies. The predicted LULC for the year 2026 is shown in Fig. 6 (bottom). In the accuracy assessment, the overall accuracy is obtained as $(41 + 40 + 39 + 47 + 28 + 33)/282 * 100 = 79.25\%$ and the corresponding Kappa coefficient as 0.78 which is in the acceptable range.

The distribution of LULC (Km²) is compared for the years 1996, 2016 and 2026 and is shown in Table 3. It is evident that in the study region crop land (26–35%) and built area (17–30%) are highest and lowest by dense forest from the year 1996–2026. Built-up area increased to 12.9% and crop land decreases at 8.7% from 1996 to 2026 in the study region.

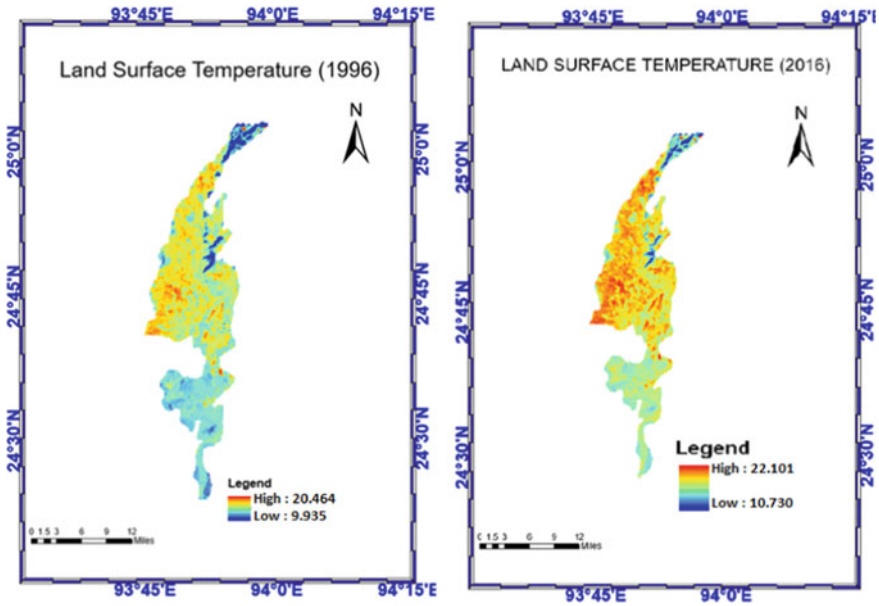


Fig. 5 Land surface temperature in the years 1996 (left) and 2016 (right)

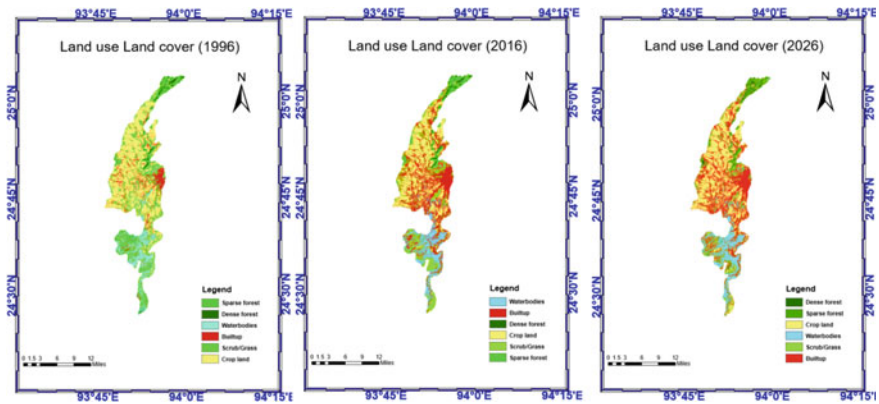


Fig. 6 LULC for 1996 (left), 2016 (right) and 2026 (bottom)

5.6 Estimated Carbon Stock and Sequestration

The amount of carbon stocks of the years 1996 (Fig. 7 left), 2016 (Fig. 7 right) and 2026 (Fig. 7 bottom). It ranges from 0 to maximum 26.6 mg of C for the year 1996 and 23.13 mg of C for the year 2016 and 21.27 mg of C for the year 2026 respectively.

Table 3 Distribution of LULC in 1996, 2016 and 2026

LULC types	1996		2016		2026 (future)		Total change (%)	
	Km ²	%	Km ²	%	Km ²	%	1996–2016	1996–2026
Dense forest	20.3	3.6	19.7	3.5	17.9	3.2	-0.1	-0.4
Sparse forest	40.0	7.2	36.6	6.6	38.2	6.8	-0.6	-0.4
Crop land	194.9	34.9	165.5	29.7	146.4	26.2	-5.3	-8.7
Scrub/Grass	136.2	24.4	112.9	20.2	116.1	20.8	-4.2	-3.6
Built-up	96.5	17.3	152.3	27.2	168.3	30.2	+9.9	+12.9
Water bodies	70.0	12.5	72.0	12.8	71.1	12.8	+0.3	+0.2

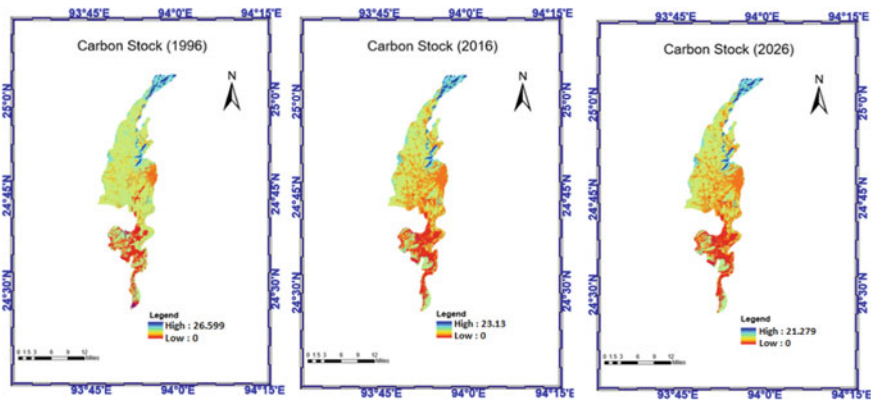
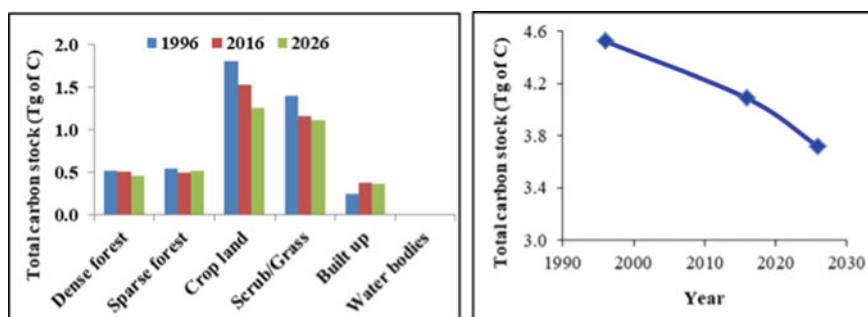


Fig. 7 Estimated carbon stock for 1996 (left), 2016 (right) and 2026 (bottom)

Table 4 representing the amount of carbon stock for each class for different years. As shown in Table 4 for the year 1996 carbon stock has been calculated as dense forest (11.55%), sparse forest (12.04%), crop land (40.07%), scrub/grass (31.01%), built-up (5.33%), and water bodies (0%). For the year 2016 it is as dense forest (12.4%), sparse forest (12.19%), crop land (37.65%), scrub/grass (28.44%), built-up (9.32%), and water bodies (0%) while the total of carbon stock is 4086645 Mg of C. In 2026 and percentage of carbon stock is as dense forest (12.36%), sparse forest (13.97%), crop land (33.95%), scrub/grass (30.01%), built-up (9.71%), and water bodies (0%) and the total is 3717033 Mg of C. Carbon stocking capacity is changing due to different parameters and Fig. 8 (right) shows comparison carbon stock value in different period while Fig. 7 (right) shows the decreasing trend from 1996 to 2026 (19.72%). Predicted carbon sequestration for the year 2026 is presented in Fig. 9. The southern part of the district has greater potential carbon sequestration than the northern part; however, this region as a whole has low carbon sequestration capacity (range 0 to -1.850).

Table 4 Estimated total carbon stock (Tg of C) for different LULC of 1996, 2016 and 2026

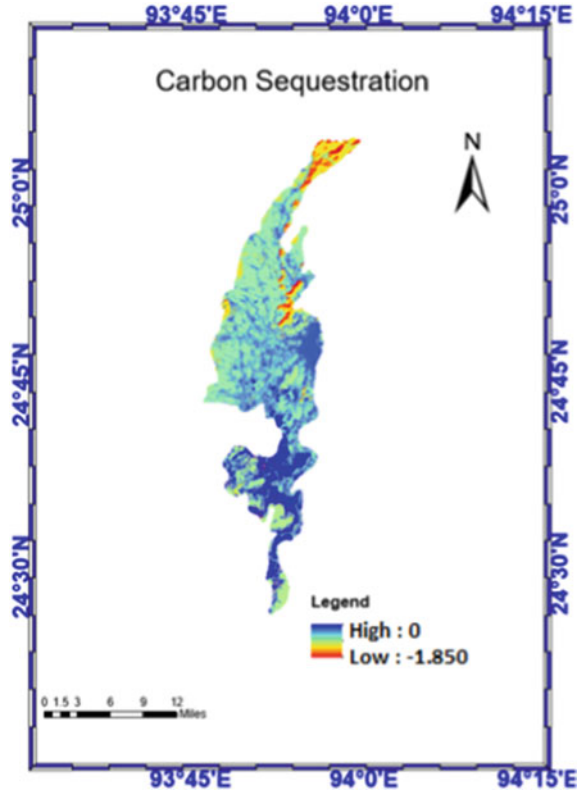
LULC types	Carbon value (Mg/hect)	1996		2016		2026	
		Tg of C	%	Tg of C	%	Tg of C	%
Dense forest	257	0.522	11.6	0.506	12.4	0.460	12.4
Sparse forest	136	0.544	12.0	0.498	12.2	0.519	14.0
Crop land	93	1.813	40.1	1.539	37.7	1.262	33.9
Scrub/grass	103	1.403	31.0	1.62	28.4	1.116	30.0
Built-up	25	0.241	5.3	0.381	9.3	0.361	9.7
Water bodies	0	0.000	0.0	0.000	0.0	0.000	0.0
Total		4.523	100	4.087	100	3.717	100

**Fig. 8** Comparison of carbon stock value (Tg) for different years (left) and changes in carbon stock from 1996 to 2026 (right)

6 Conclusions

The study region has poor potential for carbon stock as well as its sequestration as this region is rapidly urbanizing (built-up area increases at 13% approximately from 1996 to 2026). Thus, the amount of carbon stock is decreasing at 19.72% from 1996 to 2026. As forest area have an enormous change in carbon holding capacity, conservation or afforestation of forest area will help in maintaining the carbon stock in the region.

Fig. 9 Predicted carbon sequestration for the year 2026



References

1. Meena A, Bidalia A, Hanief M, Dinakaran J, Rao KS (2019) Assessment of above- and below-ground carbon pools in a semi-arid forest ecosystem of Delhi, India. *Ecol Process* 8:8. <https://doi.org/10.1186/s13717-019-0163-y>
2. Schulze ED, Sierra CA, Egenolf V, Woerdehoff R, Irslinger R, Baldamus C, Stupak I, Spellmann H (2020) The climate change mitigation effect of bioenergy from sustainably managed forests in Central Europe. *GCB Bioenergy* 12:186–197. <https://doi.org/10.1111/gcbb.12672>
3. Hou D (2021) Sustainable soil management and climate change mitigation. *Soil Use Manage* 37(2):220–223. <https://doi.org/10.1111/sum.12718>
4. Ramachandran A, Jayakumar S, Haroon RM, Bhaskaran A, Arockiasamy DI (2007) Carbon sequestration: estimation of carbon stock in natural forests using geospatial technology in the Eastern Ghats of Tamil Nadu, India. *Curr Sci* 92(3):323–331
5. Xiang S, Wang Y, Deng H, Yang C, Wang Z, Gao M (2022) Response and multi-scenario prediction of carbon storage to land use/cover change in the main urban area of Chongqing, China *Ecol Indic* 142:109205. <https://doi.org/10.1016/j.ecolind.2022.109205>
6. Martín JAR, Fuentes JA, Gonzalo J, Gil C, Miras JJR, Grau JMC, Boluda R (2016) Assessment of the soil organic carbon stock in Spain. *Geoderma* 264(A):117–125. <https://doi.org/10.1016/j.geoderma.2015.10.010>

7. Lan Z, Zhao Y, Zhang J, Jiao R, Khan MN, Sial TA, Si B (2021) Long-term vegetation restoration increases deep soil carbon storage in the Northern Loess Plateau. *Sci Rep* 11:13758. <https://doi.org/10.1038/s41598-021-93157-0>
8. Ray R, Mandal SK, González AG, Pokrovsky OS, Jana TK (2021) Storage and recycling of major and trace element in mangroves. *Sci Total Environ* 780:146379. <https://doi.org/10.1016/j.scitotenv.2021.146379>
9. Feng ZJ, Kun C, Xing PG, Smith P, Qing LL, Hui ZX, Wei ZJ, Jun HX, Ling DY (2011) Perspectives on studies on soil carbon stocks and the carbon sequestration potential of China. *Chinese Sci. Bull.* 56:3748–3758. <https://doi.org/10.1007/s11434-011-4693-7>
10. Roelofse C, Alves TM, Gafeira J, Omosanya K (2019) An integrated geological and GIS-based method to assess caprock risk in mature basins proposed for carbon capture and storage. *Int J Greenh Gas Control* 80:103–122. <https://doi.org/10.1016/j.ijggc.2018.11.007>
11. Li J, Wang Y (2019) Carbon sequestration service flow in the Guanzhong-Tianshui economic region of China: How it flows, what drives it, and where could be optimized? *Ecol Indic* 96:548–558. <https://doi.org/10.1016/j.ecolind.2018.09.040>
12. Sharma DP, Singh M (2010) Assessing the carbon sequestration potential of subtropical pine forest in North-western Himalayas—a GIS approach. *J Indian Soc Remote Sens* 38:247–253. <https://doi.org/10.1007/s12524-010-0031-9>
13. Xu X, Xu P, Zhu J, Li H, Xiong Z (2022) Bamboo construction materials: carbon storage and potential to reduce associated CO₂ emissions. *Sci Total Environ* 814:15269725. <https://doi.org/10.1016/j.scitotenv.2021.152697>
14. Bordoloi R, Das B, Tripathi OP, Sahoo UK, Nath AJ, Deb S, Das DJ, Gupta A, Devi NB, Charturvedi SS, Tiwari BK, Paul A, Tajo L (2022) Satellite based integrated approaches to modelling spatial carbon stock and carbon sequestration potential of different land uses of Northeast India. *Environ Sustain Indic* 13:100166. <https://doi.org/10.1016/j.indic.2021.100166>